Quantifying the Amount of Ice in Cold Tropical Cirrus Clouds

Melody A. Avery[1,*], D. M. Winker[1], A. Garnier[2], R. P. Lawson[3]. A. Heymsfield[4],
Q. Mo[3], M. Schoeberl[5], S. Woods[3], S. Lance[3], S. Young[6], M. Vaughan[1], C. Trepte[1]
[1]NASA/LARC, Hampton, VA; [2]SSAI, Hampton, VA, [3]SPEC, Inc., Boulder, CO,
[4]NCAR, Boulder, CO; [5]STC, Columbia, MD, [6]CSIRO/MAR, Aspendale, VIC, Australia

1. INTRODUCTION

How much ice is there in the Tropical Tropopause layer, globally? How does one begin to answer that question? Clouds are currently the largest source of uncertainty in climate models, and the ice water content (IWC) of cold cirrus clouds is needed to understand the total water and radiation budgets of the upper troposphere and lower stratosphere (UT/LS). The Cloud-Aerosol Lidar and Infrared Pathfinder Satellite Observation (CALIPSO) satellite, originally a "pathfinder" mission only expected to last for three years, has now been operational for more than eight years. Lidar data from CALIPSO can provide information about how IWC is vertically distributed in the UT/LS, and about inter-annual variability and seasonal changes in cloud ice. However, cloud IWC is difficult to measure accurately with either remote or *in situ* instruments because IWC from cold cirrus clouds is derived from the particle cross-sectional area or visible extinction coefficient. Assumptions must be made about the relationship between the area, volume and density of ice particles with various crystal habits. Recently there have been numerous aircraft field campaigns providing detailed information about cirrus ice water content from cloud probes. This presentation evaluates the assumptions made when creating the Cloud-Aerosol Lidar with Orthogonal Polarization (CALIOP) global IWC data set, using recently reanalyzed aircraft particle probe measurements of very cold, thin TTL cirrus from the 2006 CR-AVE.

----
*Corresponding author: Melody Avery
melody.a.avery@nasa.gov, 757-864-5522

2. CLOUD ICE WATER CONTENT PARAMETERIZATION

Cloud ice water content is created in the CALIOP data set using a two-step process. As an elastic backscatter lidar, CALIOP measures attenuated backscatter, and extinction is retrieved using the method of Young and Vaughan (2009). Retrieving extinction for thin subvisible cirrus requires the assumption of extinction to backscatter coefficient ratio, currently 25 sr used in the CALIOP Version 3 algorithm. Given the retrieved extinctions, Version 3 uses an empirically based power law:

$$IWC = a\sigma^b, \text{ a=119, b=1.22} \qquad (1)$$

This power law is based on a set of *in situ* and remote aircraft-based measurements (Heymsfield et. al., 2005).

Figure 1 illustrates these steps for an overpass of Hurricane Sandy, from total 532 nm backscatter, to extinction and then IWC. (Note - The differing tropical (LHS) and extra-tropical (RHS) ice cloud morphology of the Tropical and extratropical sections of Sandy is evident in this series of plots.)
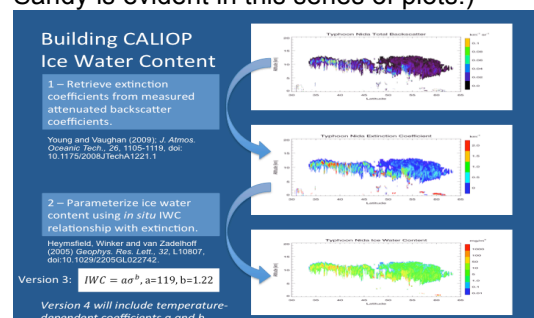

Figure 1: Representation of the CALIOP ice water content parameterization process.

3. ICE PARTICLES IN THE TTL

Ice clouds in the Tropopause Transition Layer (TTL) are difficult to measure because they are thin and most are sub-visible. The TTL is the region where vertical motion transitions between convection and the large-scale Hadley circulation. Figure 2 a, b and c show the subtle boundary between the level of neutral buoyancy with maximum convective outflow and the TTL at 14.5 km (in a) or 355 K potential temperature (in b). These plots show data from a representative month (December 2009).
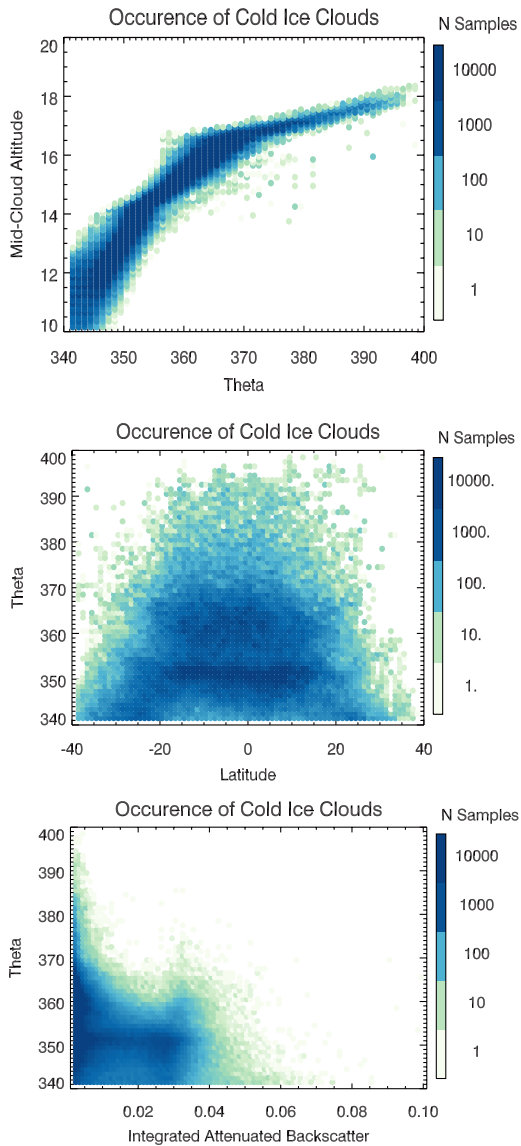
Figure 2,a-c: Occurrence of Cold Ice Clouds during December 2009. Shown are a) Potential temperature (theta) vs. mid-cloud altitude, b) Zonal cloud occurrence profile

(theta y-axis), c) Integrated attenuated backscatter in the tropics as a function of altitude (theta).

As shown in 2c, most TTL cirrus are quite thin. Volume depolarization greater than 0.05 indicates that these layers are not aerosols. Figures 3a and 3b show the distribution of ice water path, depolarization and backscatter color ratio for TTL Ci. The statistics are noisy because the sub-visible Ci are thin. Nonetheless, they provide information about this critical region when averaged appropriately.
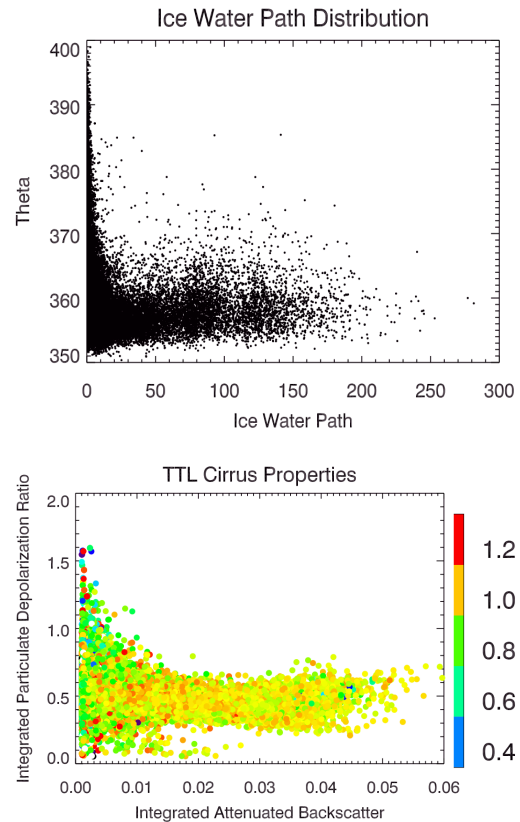
Figures 3a and 3b: Cloud ice water path as a function of theta, and depolarization as a function of integrated backscatter, colored by 1064/532 nm color ratio (color scale).

Figures 4a and 4b show the mean IAB and relative uncertainty for IAB and OD in very cold TTL clouds. Below -75 the uncertainty is dominated by the difficulty of detecting thin layers accurately. Note that we define "cold" clouds as having mid-layer temperature < -55°C, but when selected dynamically (theta > 355 K) the cloud mid-layer temperature < -65°C.

Mean Integrated Attenuated Backscatter
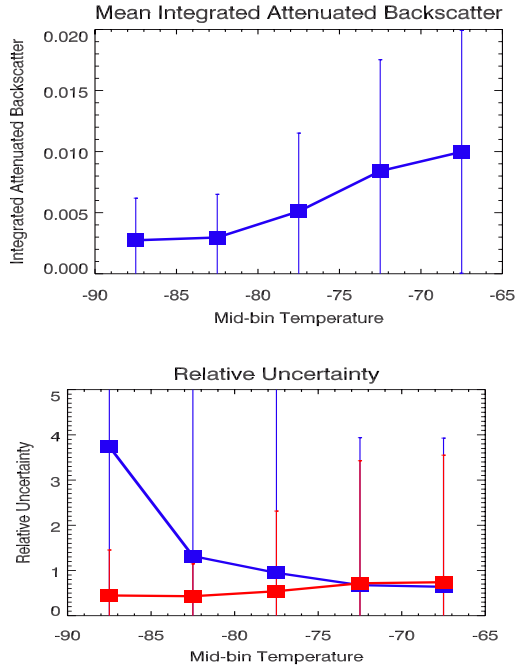

Relative Uncertainty

Figure 4a is a plot of integrated backscatter as a function of mid-cloud temperature, showing that clouds become thinner at cold temperatures in the TTL. Figure 4b shows the relative uncertainty for optical depth (red) and integrated backscatter (blue).

4. CONVECTIVE INFLUENCE ON LOWER STRATOSPHERIC WATER VAPOR

A model test, CALIOP space-based lidar and *in situ* aircraft observations all demonstrate that convective transport of water vapor and ice to the Tropical Tropopause Layer (TTL) and lowermost stratosphere is a significant process. Figures 5a and 5b show results from a simple cloud model that is added to a global domain-filling forward trajectory model (Schoeberl and Dessler, 2012) to test the impact of convectively lofted cloud ice and water vapor on the TTL and lowermost stratosphere. Results suggest that the anvil ice is needed to match CALIOP observations.
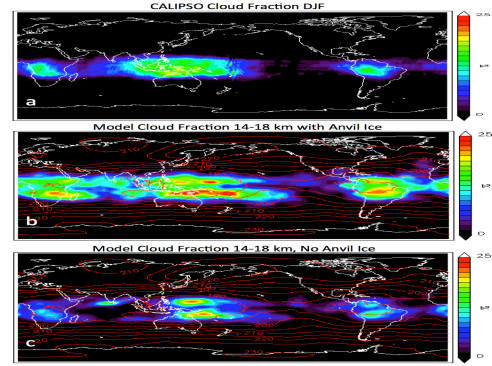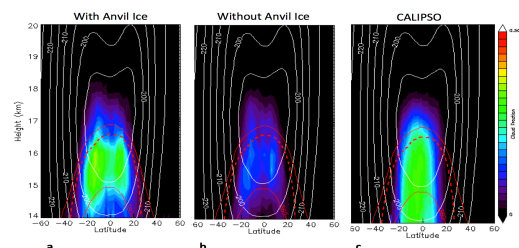

Figure 5: From Schoeberl et al., 2014, shows the global distribution of CALIOP clouds for DJF 2008-9. The trajectory model is compared to the measurements, with and without MERRA anvil ice added to a simple cloud model.

CALIOP ice water content for winter 2008-9 shown in Figure 6 as an example of how much ice mass there is at high altitudes.
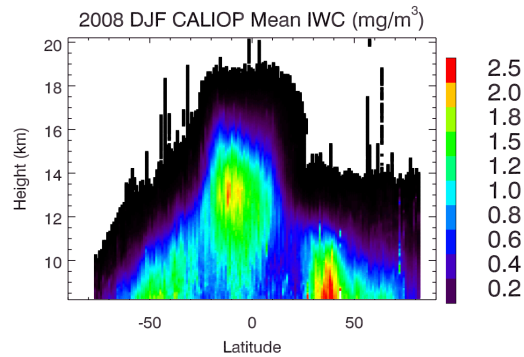

Figure 6: CALIOP zonally averaged ice water content during DJF 2008-9. Some of the apparent "noise" is due to less frequent overpasses at low latitudes.

Measurements of cloud microphysical parameters in the TTL are few. Figure 7 shows flight tracks from the CR-AVE mission out of Costa Rica in JF 2006.
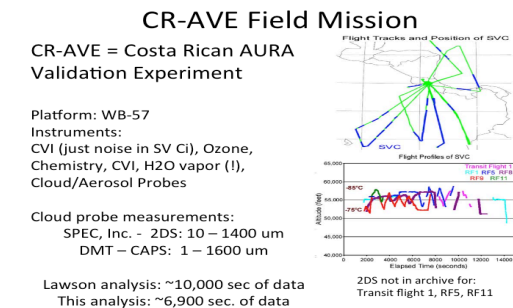

Figure 7: Flight tracks from CR-AVE

A SPEC, Inc. optical array probe (2D-S) measured the particle size distributions, extinctions and IWC in the TTL and lowermost stratosphere from the WB-57. IWC measurements are shown in Figure 8.
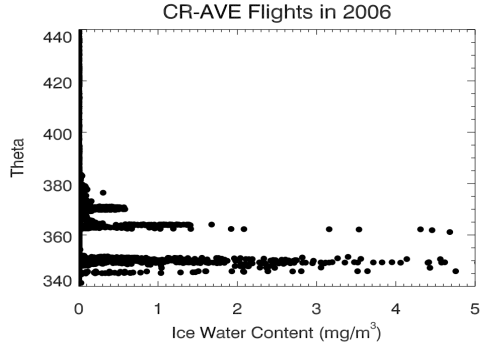

Figure 8: SPEC 2D-S IWC composite

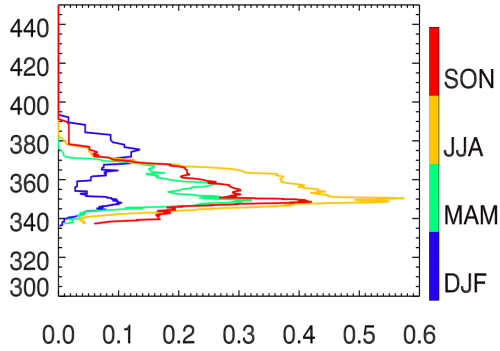Figure 9 shows the corresponding CALIOP cloud fraction climatology.

Figure 9: Cloud fraction, San Jose Costa Rica, DJF 2008-2012.

An interesting result from CR-AVE is that there is more IWC at the cold point, but the largest particles occur above 380 K in the lowermost stratosphere.
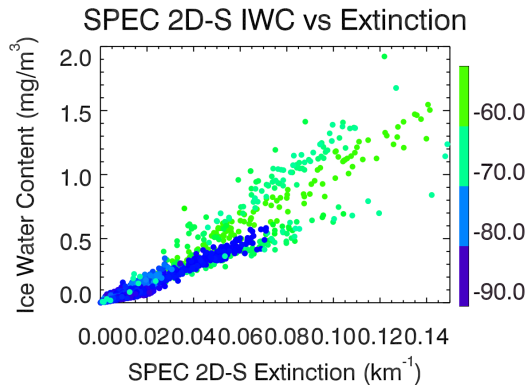

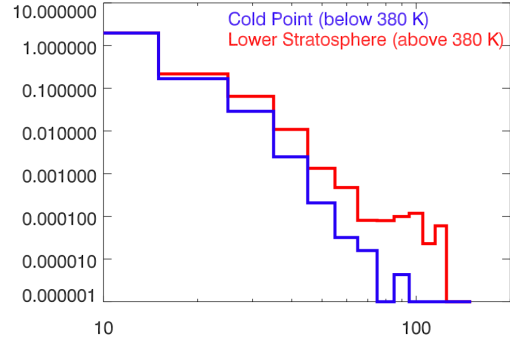Figure 10: CR-AVE 2D-S IWC vs. Extinction

Figure 11: Average particle size distribution in the TTL measured by the 2D-S

These size distributions agree well with the observations of de Reus et al., 2009, from Darwin during SCOUT. Typical CPI images of these particles are shown in Figure 12.

Figure 12: SPEC CPI images of ice particles in the lowermost stratosphere during CR-AVE.

5. EVALUATING EXTINCTION COEFFICIENTS

A new compilation of extinction coefficients measured using aircraft particle probes (details in Heymsfield et. al., 2014) has been evaluated, and statistics of the distribution are shown in Figure 14a, in blue. The mean extinction clearly decreases at colder temperatures, as will the associated ice water content. CALIOP data is shown in black for all of the data, and in red for constrained (QC=1) extinction solutions. Plot 14b shows that the constrained extinctions are not representative of the ensemble of CALIOP extinctions within each temperature range, and that at cold

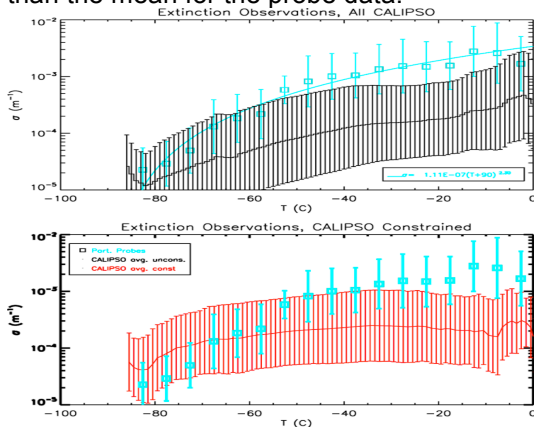temperatures the CALIOP mean is larger than the mean for the probe data.

Figure 14a and b: In situ measured extinction coefficients (blue) compared with CALIOP retrieved extinctions - all (black) and only constrained solutions (red).

Figure 15 shows that for temperatures colder than -55 deg C, constrained solutions are 20% or less of the data.
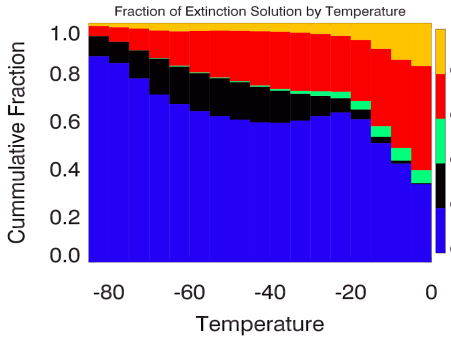

Figure 15: CALIOP distribution of extinction solution types as a function of temperature. Most cold Ci clouds are transparent to CALIOP and unconstrained (blue); these will be assigned an a priori value of the lidar ratio to solve for σ.

Figures 15 a and b show median integrated backscatter and extinctions as a function of temperature. The green line on plot d) is made by increasing the default lidar ratio from 25 to 32.
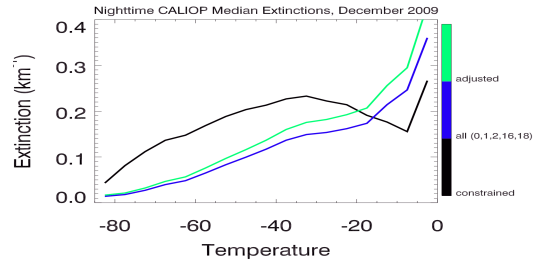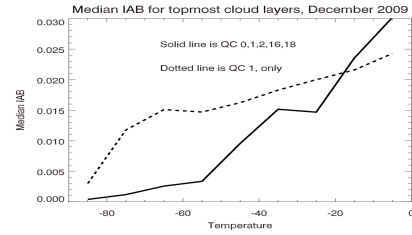

Figure 15: a) IAB and b) Extinction as a function of temperature.

6. COMPARISON WITH IIR

A matched set of CALIOP and IIR data from December, 2009 (as in Parts II and II) is used for comparison between IIR and CALIOP retrievals of cloud layer optical depth, effective diameter and ice water path. The layers were selected to optimize the IIR retrievals with these characteristics: single (topmost) transparent (to CALIOP) cloud layers of IIR scene types 21, 30 and 24 (see Garnier 2013) with measured reference radiances. These layers were then further classified as: 1 – Cold: centroid temperatures < -55 deg C (30k samples);
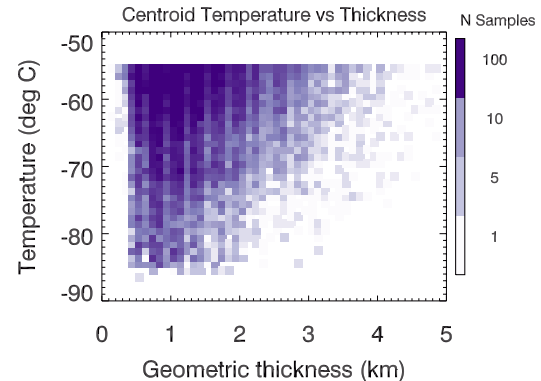2 – TTL: cloud bases > 14.5 km (6k samples)

Figure 16a: Occurrence of layer geometric thickness as a function of temperature for "cold" ice clouds (T < -55 deg C)
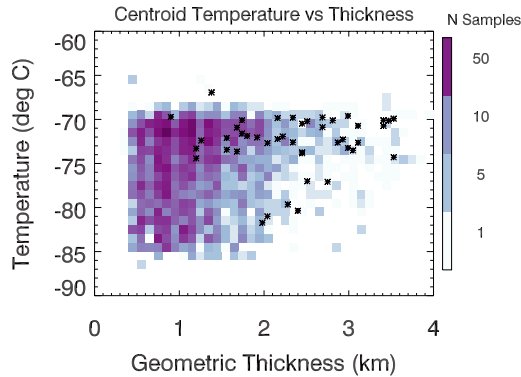
Figure 16b: As for 16a, but TTL layers only.

In the month of December, 2009 there were only 44 Ci layers with constrained CALIOP retrievals in the TTL. These data points are labeled with crosses on Figures 16b, 17b and 18b. CALIOP optical depth is in general lower than the equivalent IIR optical depth because the unconstrained retrievals are assigned a lidar ratio of 25 that is too low for these thin clouds. But for layers with small integrated backscatter, the constrained optical depths appear to be much higher than the IIR, suggesting that the retrieved lidar ratios are too high for weakly scattering cloud layers, or that the IIR optical depths are too low for these clouds.
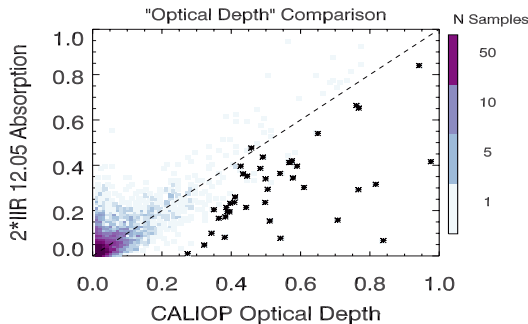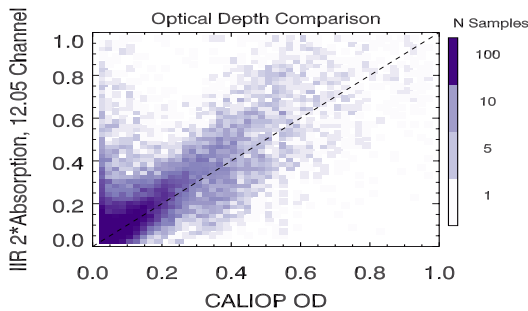

Figures 17a and 17b: 2*IIR 12.05 μm optical depth compared with the CALIOP optical depth (layer integrated extinction) for "cold" and "TTL" ice clouds, respectively.

We evaluated effective diameter as it is defined in Mitchell (2010):

$$D_{eff} = (3/\rho_{ice})(IWC/\sigma) \quad (2)$$

In this case we are using integrated quantities for the cloud layers, so the ratio is ice water path (IWP) to optical depth. CALIOP effective diameters are larger than those from the IIR, which may indicate that the Version 3 IWC parameterization is too large for colder temperatures. New analysis in Heymsfield et al., 2014 suggests updated IWC parameterizations that are currently being evaluated for possible use in CALIOP Version 4.
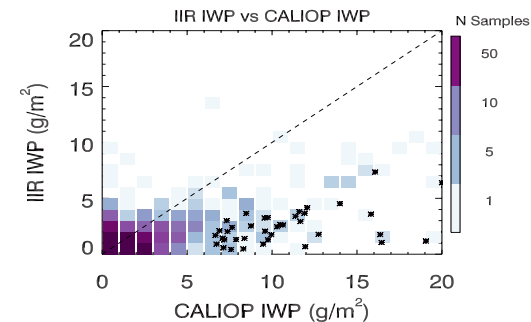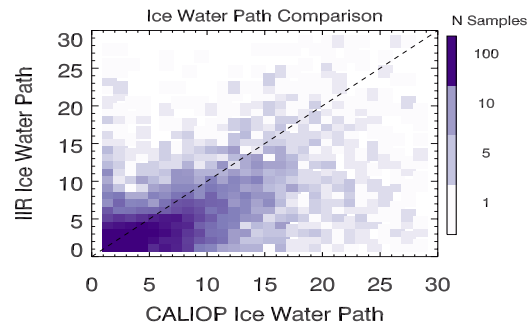
Figures 18a and 18b: IIR vs. CALIOP cloud ice water path for "cold" and "TTL" ice clouds.

Figures 18 a and b show that the IIR and CALIOP ice water path for cold and TTL Ci clouds agrees fairly well, with CALIOP slightly higher even while having low optical depths, so the differences apparently cancel each other somewhat. The CALIPSO team is currently evaluating lidar ratios and iwc parameterizations for the new Version 4 Level 2 product.

6. REFERENCES

Avery, M., D. Winker, A. Heymsfield, M. Vaughan, S. Young, Y. Hu and C. Trepte (2012), "Cloud ice water content retrieved from the CALIOP space-based lidar", *Geophys. Res. Let.,* **39**, doi:10.1029/2011GL050545.

de Reus, M., S. Borrmann, A. Bensemer, A. J. Heymsfield, R. W. Weigel, C. Schiller, V. Miltev, W. Frey, D. Kunkel, A. Kurten, J. Curtius, N. M. Sitnikov, A. Ulanovsky, F. Ravegnani, 2009: "Evidence for ice particles i the tropical stratosphere from in-situ measurements", *Atmos. Chem. Phys.*, **9**, pp. 6775-6792.

Fernald, F. G., B. M. Herman and J. A. Regan, (1972): "Determination of aerosol height distributions by LIDAR", *J. Applied Met.* 11**,** pp. 482-489.

Garnier, A., J. Pelon, P. Dubuisson, M. Faivre, O. Chomette, N. Pascal, and D. Kratz (2012), "Retrieval of cloud properties using CALIPSO imaging infrared radiometer, Part 1: Effective emissivity and optical depth", *J. Ap. Met. And Clim.,* **51***,* doi:10.1175/JAMC-D-11-0220.1.

Garnier, A., J. Pelon, P. Dubuisson, P. Yang, M. Faivre, O. Chomette, N. Pascal, P. Lucker, T. Murray (2013): "Retrieval of cloud properties using CALIPSO imaging infrared radiometer, Part 2: Effective diameter and ice water path", *J. J. Ap. Met. And Clim.,* **52***,* doi:10.1175/JAMC-D-12-0328.1.

Heymsfield, A. D., Winker and G.-J. van Zadelhoff (2005), "Extinction-ice water content-effective radius algorithms for CALIPSO", *Geophys. Res. Lett.,* **32**, L10807, doi:10.1029/2205GL022742.

Heymsfield, A. D., D. M. Winker, M. A> Avery, M. A. Vaughan, G. Diskin, M. Deng, V. Mitev (2013): "Relationships between Ice Water Content and Volume Extinction Coefficient from In Situ Observations for Temperatures from 08 to 2868C: Implications for Space borne Lidar Retrievals", *J. Applied Meteorol. Clim.,* 10.1175/JAMC-D-13-087.1.

Hunt, W. H., D. M. Winker, M. A. Vaughan, K. A. Powell, P. L. Lucker, C. Weimer (2009): "CALIPSO lidar description and performance assessment", *J. Atm. Oceanic Tech.,* **26**, pp. 1214-1228, doi: 10.1175/2009JTECHA1223.1.

Lawson, R. P., B. Pilson, B. Baker, Q. Mo, E. Jensen, L. Pfister, P. Bui (2008): "Aircraft measurements of microphysical properties of subvisible cirrus in the tropical tropopause layer", *Atmos. Chem. Phys.,* **8**, 1609-1620.

Mitchell, D. L., R. P. D'Entremont, R. P. Lawson, (2010): "Inferring cirrus size distributions through satellite remote sensing and microphysical databases", *J. Atmos. Sci.,* **67**, 1106-1125.

Platt, C. M. R., S. A. Young, R. T. Austin, G. R. Patterson, D. L. Mitchell, S. D. Miller (2002): LIRAD Observations of tropical cirrus clouds in MCTEX. Part I: Optical properties and detection of small particles in cold cirrus, *J. Atmos. Sci.,* **59(22)**, 3145-3162, doi: 10.1175/JAS2843.

Schmitt, C. G. and A. J. Heymsfield (2009): "The size distribution and terminal-weighted velocity of low-latitude tropical cirrus cloud populations", *J. Atm. Sci.,* **66,** 2013-2028.

Schoeberl, M., A. Dessler, T. Wang, M. Avery, E. Jensen (2014): "Cloud Formation, Convection, and Stratospheric Dehydration", submitted to *Earth and Space Sciences.*

Winker, D. M., M. A. Vaughan, A. H. Omar, Y. Hu, K. A. Powell, Z. Liu, W. H. Hunt, and S. A. Young, 2009: "Overview of the CALIPSO Mission and CALIOP Data Processing Algorithms", *J. Atmos. Oceanic Technol.*, **26**, 2310–2323, doi:10.1175/2009JTECHA1281.1.

Young, S. and M. Vaughan (2009), "The Retrieval of Profiles of Particulate Extinction from Cloud-Aerosol Lidar Infrared Pathfinder Satellite Observations (CALIPSO) Data: Algorithm Description", *J. Atmos. Oceanic Tech.,* **26**, 1105-1119, doi: 10.1175/2008JTechA1221.1

Young, S. and M. Vaughan, R. Kuehn and D. Winker (2013), "The Retrieval of Profiles of Particulate Extinction from Cloud-Aerosol Lidar Infrared Pathfinder Satellite Observations (CALIPSO) Data: Uncertainty and Error Sensitivity Analyses" J. Atmos. Oceanic Technol., doi: 10.1175/JTECH-D-12-00064.1